

Photoresponsive Molecular Switch for Regulating Transmembrane Proton-Transfer Kinetics

Ying Li,[†] Edmund C. M. Tse,[†] Christopher J. Barile,[†] Andrew A. Gewirth,^{*,†,§}
and Steven C. Zimmerman^{*,†}

[†]Department of Chemistry, University of Illinois at Urbana—Champaign, 600 South Mathews Avenue, Urbana, Illinois 61801, United States

[§]International Institute for Carbon Neutral Energy Research (WPI-I2CNER), Kyushu University, Fukuoka 812-8581, Japan

S Supporting Information

ABSTRACT: To control proton delivery across biological membranes, we synthesized a photoresponsive molecular switch and incorporated it in a lipid layer. This proton gate was reversibly activated with 390 nm light (*Z*-isomer) and then deactivated by 360 nm irradiation (*E*-isomer). In a lipid layer this stimuli responsive proton gate allowed the regulation of proton flux with irradiation to a lipid-buried O₂ reduction electrocatalyst. Thus, the catalyst was turned on and off with the *E*-to-*Z* interconversion. This light-induced membrane proton delivery system may be useful in developing any functional device that performs proton-coupled electron-transfer reactions.

Precisely regulated proton transfer is essential to many biological reactions and alternative energy schemes that involve redox reactions with one or more proton-coupled electron-transfer (PCET) steps.^{1–4} As one example, the oxygen reduction reaction to form water (ORR: O₂ + 4e[−] + 4H⁺ → 2H₂O) is critical to sustaining life on earth.^{5,6} Cytochrome *c* oxidase (CcO) and laccase are two enzymes that evolved to develop intricate proton transport chains which provide exquisite control over the kinetics of proton delivery to the ORR active site.^{7–11}

The mechanisms associated with multi-step PCET reactions are difficult to decipher because of the intricate interplay between the thermodynamics and kinetics of electron and proton transfer.^{2–4,12} The use of a self-assembled monolayer (SAM) can decouple the kinetics and thermodynamics of electron transfer, the latter dictated by the electrode potential.^{13,14} We recently developed a new experimental framework using a hybrid bilayer membrane (HBM) to delineate the relative importance of the kinetics and thermodynamics of proton transfer to a system that catalyzes PCET reactions.^{15,16} A HBM consists of a SAM with a monolayer of lipid appended on top.¹⁷ In one embodiment, a dinuclear Cu molecular ORR catalyst (CuBTT: Cu complex of 6-((3-(benzylamino)-1,2,4-triazol-5-yl)amino)hexane-1-thiol) forms the SAM.¹⁶ We previously demonstrated that the spontaneous flip-flop diffusion of lipid-bound aliphatic acids function as a pH-sensitive switch turning on and off transmembrane proton delivery to the catalyst.¹⁵ The proton delivery via this flip-flop diffusion of the proton carriers occurs spontaneously in the presence of a pH gradient.^{18,19} It can be

advantageous to regulate the proton-transfer kinetics more precisely without the associated perturbation in proton thermodynamics that arises with a pH change.

To avoid concomitant changes in proton thermodynamics while modulating the proton kinetics, natural systems utilize light to execute an additional level of control over proton and electron-transfer steps by having specific functional groups that adopt precise photoinduced conformational changes. For example, a 5 Å movement of an ubiquinone moiety accompanied by a 180° propeller twist of an isoprene chain upon illumination in the photosynthetic reaction center of *Rhodobacter sphaeroides* is a necessary prerequisite to proton uptake for photosynthesis that involves PCET steps.²⁰ The intricate photoregulation of proton transport in nature has inspired a tremendous amount of effort toward mimicking these natural systems on the macromolecular level.²¹ Although artificial photosynthetic reaction centers have been developed in the past decades,^{22,23} the photoregulation of transmembrane proton kinetics without involving fluctuations in electron transfer or proton thermodynamics to our best knowledge has not been achieved with a single-component small molecular system.

A HBM with a photoresponsive proton carrier could mimic the light-induced conformational gating found in nature and afford a new approach to tune transmembrane proton-transfer kinetics with temporal and spatial control. Further, such a system could eliminate the need for chemical inputs that invariably generates waste products. In this report, we develop a simple, artificial, membrane-bound, photoresponsive proton carrier that regulates proton kinetics across a lipid membrane. The new proton carrier (**BA**) features a boronic acid headgroup for proton transfer, a stiff stilbene body for photoresponsiveness, and an alkyl tail for lipid incorporation. Boronic acids typically exhibit pK_a values of ca. 9,²⁴ a feature that ensures the proton carrier to be mostly in the neutral form in pH 7 solution. The ability of **BA** to cycle between two photo-distinguishable states allows us to construct a proof-of-concept, light-addressable transmembrane proton kinetics regulator in a HBM platform without perturbing the proton thermodynamics in the bulk solution.

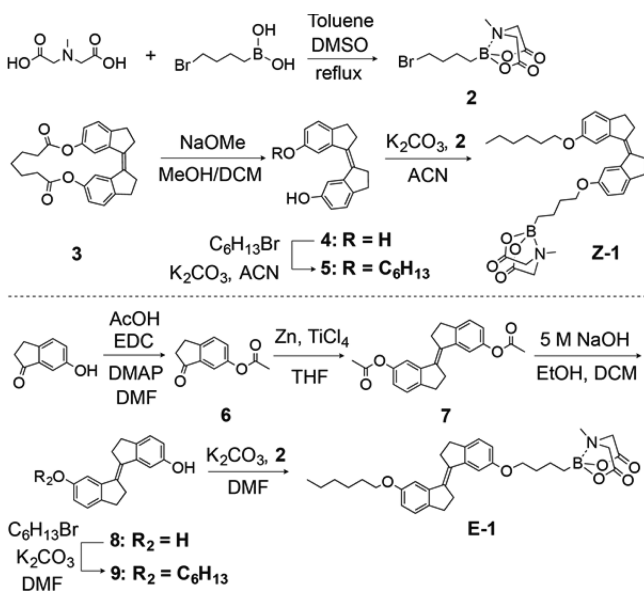
Received: September 23, 2015

Published: October 29, 2015

Like many other photoresponsive chromophores,^{25,26} a stiff stilbene moiety (1,1'-biindane) has either a *Z* or *E* configuration with respect to its central double bond upon photoisomerization.^{27–29} This chromophore has garnered increasing attention because of its scalable synthesis, easy derivatization, lack of thermal relaxation at room temperature, high quantum yield (50%) for *E*-to-*Z* photoisomerization, and quantitative *Z*-to-*E* reversion.^{27–32} The stiff stilbene moiety has been applied as a light driven internal molecular force probe.^{31,32} Nevertheless, the proton-gating ability of functional materials based on stiff stilbene remains largely unexplored.

We first prepared both the *Z*- and *E*-forms of the protected photoresponsive switch, the synthesis beginning from the photoreactive core, followed by the sequential installation of the alkyl tail and the protected acid headgroup (see Scheme 1

Scheme 1. Preparation of the Protected Photoswitch Molecules: Z-1 and E-1



and Supporting Information for details). The trivalent *N*-methyliminodiacetic acid (MIDA) ligand, developed by Burke and co-workers,^{33,34} was used to avoid decomposition of the boronic acid group during the synthesis. Indeed, the MIDA boronate ester was simply prepared from commercially available starting materials, survived the harsh reaction conditions, and allowed purification by chromatography. The deprotection of Z-1 and E-1 was easily achieved at room temperature with concentrated aqueous NaOH solution to afford the two isomers Z-BA and E-BA, respectively.

The light-induced *E*-*Z* isomerization of BA was first demonstrated in solution and followed by ¹H NMR spectroscopy. Figure 1a displays the structures of E-BA and Z-BA, and highlights the protons whose resonances were followed in the ¹H NMR study. Figure 1b shows an overlay of truncated ¹H NMR spectra: Z-BA, E-BA, and one cycle of the *E*-*Z*-*E* conversion. The protons H_a and H_b in Z-BA (Figure 1b, black line) appeared at 2.88 and 2.79 ppm, respectively. Their equivalent protons H_a' and H_b' in E-BA (red line) shifted downfield to 3.15 ppm ($\Delta\delta$ [H_a] = 0.27 ppm) and 3.05 ppm ($\Delta\delta$ [H_b] = 0.26 ppm), correspondingly. Upon UV irradiation at 360 nm, about 40% of E-BA was converted into Z-BA according to the ¹H NMR integration (green line). The mixture

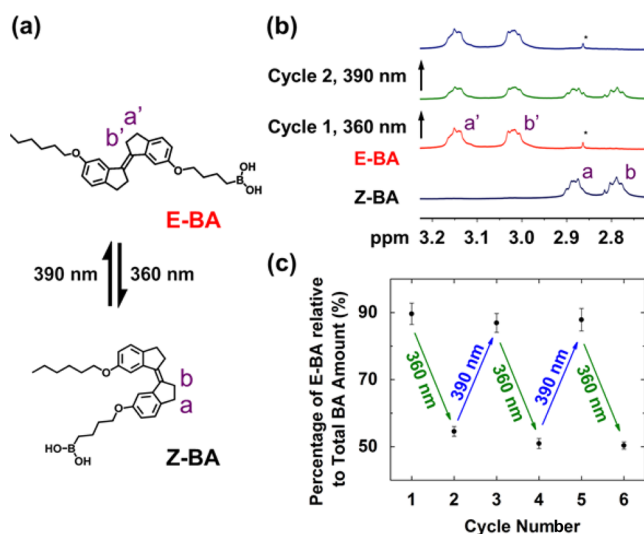


Figure 1. (a) Structures of E-BA and Z-BA with the protons of interest labeled. (b) Stacked truncated NMR spectra of BA (*Z*- and *E*-isomers) in CD₂Cl₂, indicating the corresponding proton signal shifts according to the irradiation cycles. * = ¹H resonance of the methyl group from MIDA after the deprotection step. (c) Repeated cycles of E-BA to Z-BA conversion. See Supporting Information for additional information (e.g., irradiation times).

was exposed to UV irradiation at 390 nm and the *Z*-isomer was almost quantitatively converted back to the *E*-isomer (blue line). The complete *Z*-to-*E* and partial *E*-to-*Z* stilbene photoisomerization is consistent with reported systems.^{27,28} The full isomerization cycle was repeated two more times, and similar results were obtained. Figure 1c shows the percentage of E-BA versus the total BA plotted across sequential photoirradiation events. Despite these observable changes in the ¹H NMR spectra (Figure S1), suggesting that the boronic acid group remains intact.

Having demonstrated in solution the reversible photoresponsiveness of E-BA and Z-BA, we probed their ability to act as proton carriers in a HBM. Figure 2a displays the architecture of the three HBMs with and without BA incorporated in the lipid layer. Figure 2b shows linear sweep voltammograms (LSVs) of O₂ reduction by a SAM of CuBTT covered by a DMPC monolayer with and without the proton

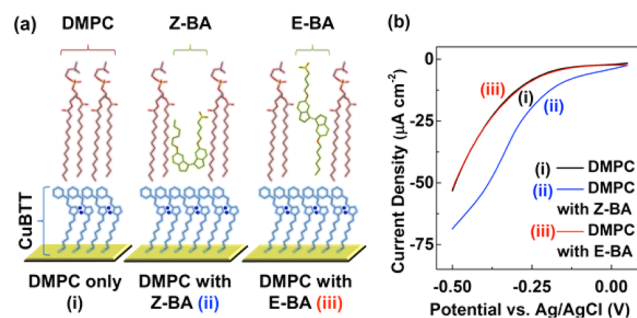


Figure 2. (a) Schematic of the HBMs studied: (i) DMPC only, (ii) DMPC with Z-BA incorporated, and (iii) DMPC with E-BA incorporated. (b) Linear sweep voltammograms, recorded at a scan rate of 10 mV/s, of O₂ reduction in O₂-saturated pH 7 buffer, catalyzed by CuBTT covered by a monolayer of DMPC (black) with Z-BA (blue) or E-BA (red) incorporated in the lipid layer.

carriers added. In the absence of the proton carriers, the lipid layer blocks access of protons in the bulk solution to CuBTT inside a HBM, resulting in a background O_2 reduction current density of about $40 \mu A cm^{-2}$ at $-450 mV$ vs Ag/AgCl (Figure 2b, black line).

Upon incorporation of Z-BA, the O_2 reduction current density at $-450 mV$ increases by about 60% (blue line), indicating that Z-BA delivers protons from the bulk solution across the lipid layer to the CuBTT catalyst for O_2 reduction as has been demonstrated previously for other proton carriers in HBM systems.^{15,16} However, the O_2 reduction current density with E-BA added to the lipid layer (red line) is the same as the lipid-only case, signifying that E-BA is unable to transport protons across the hydrophobic lipid layer. The different behavior of E-BA and Z-BA is likely not a result from a change in pK_a because analogous carboxylic acids exhibit similar pK_a values (Figure S2). We propose that the effect originates from the different lengths of the two isomers in the phospholipid. When the proton carrier isomerizes from E to Z, it decreases in length by $\sim 10 \text{ \AA}$ and reduces the van der Waals interactions between the proton carrier and the phospholipids.^{35,36} Thus, we suggest that, relative to the E-isomer, the Z-isomer has a lower energy barrier for transmembrane flip-flop diffusion and thus induces proton delivery.

We next explore the photoswitching behavior of E-BA and Z-BA in a HBM. Figure 3a displays a set of LSVs of O_2 reduction

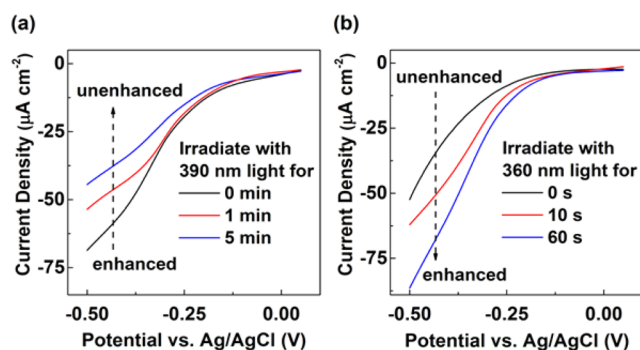


Figure 3. LSVs, recorded at a scan rate of $10 mV/s$, of O_2 reduction in O_2 -saturated pH 7 phosphate buffer, catalyzed by CuBTT covered by a monolayer of DMPC with (a) Z-BA incorporated in the lipid layer, irradiated with 390 nm light for 0 min (black), 1 min (red), and 5 min (blue), and (b) E-BA incorporated in the lipid layer, irradiated with 360 nm light for 0 s (black), 10 s (red), and 60 s (blue).

by CuBTT covered by a DMPC monolayer with Z-BA added to the lipid layer with various irradiation periods. Upon irradiation at 390 nm for 1 and 5 min, the O_2 reduction current density at $-450 mV$ drops by about 60% and 95%, respectively (Figure 3a, red and blue lines). As the irradiation time increases, the O_2 reduction current decreases until it reaches nearly the same value as the lipid-only case or the case with E-BA added to the DMPC layer. These findings indicate that as more of the proton carrier is converted to its inactive form (E-BA), fewer protons are delivered across the lipid membrane, thus resulting in less catalytic O_2 reduction current.

Figure 3b shows O_2 reduction LSVs by CuBTT covered by a DMPC monolayer with E-BA added to the lipid layer with various irradiation periods. Upon irradiation with 360 nm for 10 s, the O_2 reduction current density increases by about 65% (Figure 3b, red line). The O_2 reduction current reaches a value similar to the case with Z-BA added to the DMPC layer by

irradiating for 1 min (blue line). Although the solution studies (Figure 1) indicated that E-Z isomerization is nonquantitative, the results shown here suggest that a sufficient amount of Z-isomer is generated in the lipid layer to achieve saturation in the transmembrane proton flux. We note that the E-to-Z switching time is shorter than the Z-to-E switching time, an observation consistent with the isomerization kinetics of other stiff stilbenes.³⁷ Control experiments demonstrate that the integrity of the CuBTT SAM and the lipid layer is not compromised by irradiating with light at 360 and 390 nm (Figure S3a–c). For example, the possibility of pore formation or another defect is ruled out using $K_3Fe(CN)_6$ as a probe (Figure S3d). Furthermore, we interrogate the content of the lipid layer using ESI-MS, which confirms the presence of proton carrier in the lipid layer (Figure S4). Taken together, these results represent the first example of using a molecular switch and light to gate proton delivery across a phospholipid membrane.

We further examined light-induced proton delivery in a HBM after a complete on-off-on cycle. Figure 4 displays LSVs

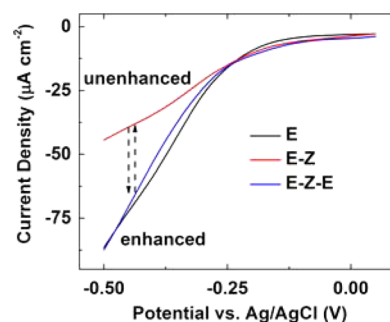


Figure 4. O_2 reduction LSVs in O_2 -saturated pH 7 phosphate buffer at a scan rate of $10 mV/s$ by CuBTT covered by a monolayer of DMPC with Z-BA incorporated in the lipid layer (black) irradiated with 390 nm light for 5 min (red) followed by 360 nm light for 1 min (blue).

of O_2 reduction by CuBTT covered by a DMPC monolayer with Z-BA incorporated after sequential irradiation. Upon irradiation at 390 nm for 5 min and then at 360 nm for 1 min, the O_2 reduction current density is revived to within 10% of the current density of the initial on-state (Figure 4, blue line), showing the reversibility of the system. 1H NMR spectra demonstrate that the slight decrease in O_2 reduction current density stems from leaching of the proton carrier from the lipid layer of the HBM into the bulk solution (Figure S5).

In summary, we have developed the first photoresponsive proton gate in a HBM and demonstrated its application by successively turning off and back on proton transfer for use in a PCET reaction without concomitant changes in solution pH. The photoswitch uses the interconversion of the Z- and E-isomer, which allows a flipping mechanism that, in turn, facilitates transmembrane proton delivery. This matching of molecular to lipid structure by modulating proton flux directly leads to the on-and-off switching of the lipid-covered O_2 reduction catalyst. We envision that by delineating the effects of proton-transfer thermodynamics and kinetics, we can further elucidate the reaction mechanism of PCET processes. Further spatial regulation of this photoresponsive proton gate in the bio-inspired HBM platform could permit the development of more complex hybrid models for future biophotonics, optoelectronics, molecular switches, and memory elements.

■ ASSOCIATED CONTENT**■ Supporting Information**

The Supporting Information is available free of charge on the ACS Publications website at DOI: 10.1021/jacs.5b10016.

Experimental procedures, NMR spectra, electrochemical data, and Figures S1–S5 (PDF)

■ AUTHOR INFORMATION**Corresponding Authors**

*agewirth@illinois.edu

*sczimmer@illinois.edu

Notes

The authors declare no competing financial interest.

■ ACKNOWLEDGMENTS

S.C.Z. acknowledges support of the National Science Foundation (NSF CHE-1307404). E.C.M.T. acknowledges a Croucher Foundation Scholarship. C.J.B. acknowledges a National Science Foundation Graduate Research Fellowship (NSF DGE-1144245) and a Springborn Fellowship. We thank the U.S. Department of Energy (DEFG02-95ER46260) for support of this research.

■ REFERENCES

- (1) Chang, C. J.; Chang, M. C. Y.; Damrauer, N. H.; Nocera, D. G. *Biochim. Biophys. Acta, Bioenerg.* **2004**, *1655*, 13–28.
- (2) Weinberg, D. R.; Gagliardi, C. J.; Hull, J. F.; Murphy, C. F.; Kent, C. A.; Westlake, B. C.; Paul, A.; Ess, D. H.; McCafferty, D. G.; Meyer, T. J. *Chem. Rev.* **2012**, *112*, 4016–4093.
- (3) Mayer, J. M.; Rhile, I. J. *Biochim. Biophys. Acta, Bioenerg.* **2004**, *1655*, 51–58.
- (4) Hammes-Schiffer, S. *Acc. Chem. Res.* **2009**, *42*, 1881–1889.
- (5) Arnold, S. *Mitochondrion* **2012**, *12*, 46–56.
- (6) Hüttemann, M.; Pecina, P.; Rainbolt, M.; Sanderson, T. H.; Kagan, V. E.; Samavati, L.; Doan, J. W.; Lee, I. *Mitochondrion* **2011**, *11*, 369–381.
- (7) Brändén, G.; Gennis, R. B.; Brzezinski, P. *Biochim. Biophys. Acta, Bioenerg.* **2006**, *1757*, 1052–1063.
- (8) Hofacker, I.; Schulten, K. *Proteins: Struct., Funct., Genet.* **1998**, *30*, 100–107.
- (9) Kirchberg, K.; Michel, H.; Alexiev, U. *Biochim. Biophys. Acta, Bioenerg.* **2013**, *1827*, 276–284.
- (10) Bento, I.; Silva, C.; Chen, Z.; Martins, L.; Lindley, P.; Soares, C. *BMC Struct. Biol.* **2010**, *10*, 28.
- (11) Silva, C. S.; Damas, J. M.; Chen, Z.; Brissos, V.; Martins, L. O.; Soares, C. M.; Lindley, P. F.; Bento, I. *Acta Crystallogr., Sect. D: Biol. Crystallogr.* **2012**, *68*, 186–193.
- (12) Mayer, J. M. *Annu. Rev. Phys. Chem.* **2004**, *55*, 363–390.
- (13) Chidsey, C. E. D. *Science* **1991**, *251*, 919–922.
- (14) Bard, A. J.; Faulkner, L. R. *Electrochemical Methods: Fundamentals and Applications*; Wiley: New York, 2000.
- (15) Barile, C. J.; Tse, E. C. M.; Li, Y.; Sobyra, T. B.; Zimmerman, S. C.; Hosseini, A.; Gewirth, A. A. *Nat. Mater.* **2014**, *13*, 619–623.
- (16) Hosseini, A.; Barile, C. J.; Devadoss, A.; Eberspacher, T. A.; Decreau, R. A.; Collman, J. P. *J. Am. Chem. Soc.* **2011**, *133*, 11100–11102.
- (17) Hosseini, A.; Collman, J. P.; Devadoss, A.; Williams, G. Y.; Barile, C. J.; Eberspacher, T. A. *Langmuir* **2010**, *26*, 17674–17678.
- (18) Schönfeld, P.; Schild, L.; Kunz, W. *Biochim. Biophys. Acta, Bioenerg.* **1989**, *977*, 266–272.
- (19) McConnell, H. M.; Kornberg, R. D. *Biochemistry* **1971**, *10*, 1111–1120.
- (20) Stowell, M. H. B.; McPhillips, T. M.; Rees, D. C.; Soltis, S. M.; Abresch, E.; Feher, G. *Science* **1997**, *276*, 812–816.

- (21) Koçer, A.; Walko, M.; Meijberg, W.; Feringa, B. L. *Science* **2005**, *309*, 755–758.
- (22) Steinberg-Yfrach, G.; Liddell, P. A.; Hung, S.-C.; Moore, A. L.; Gust, D.; Moore, T. A. *Nature* **1997**, *385*, 239–241.
- (23) Xie, X.; Crespo, G. A.; Mistlberger, G.; Bakker, E. *Nat. Chem.* **2014**, *6*, 202–207.
- (24) Hall, D. G. *Boronic Acids*; Wiley-VCH Verlag GmbH & Co. KGaA: Weinheim, Germany, 2006; pp 1–99.
- (25) Beharry, A. A.; Woolley, G. A. *Chem. Soc. Rev.* **2011**, *40*, 4422–4437.
- (26) Klajn, R. *Chem. Soc. Rev.* **2014**, *43*, 148–184.
- (27) Xu, J.-F.; Chen, Y.-Z.; Wu, D.; Wu, L.-Z.; Tung, C.-H.; Yang, Q.-Z. *Angew. Chem., Int. Ed.* **2013**, *52*, 9738–9742.
- (28) Yan, X.; Xu, J.-F.; Cook, T. R.; Huang, F.; Yang, Q.-Z.; Tung, C.-H.; Stang, P. J. *Proc. Natl. Acad. Sci. U. S. A.* **2014**, *111*, 8717–8722.
- (29) Wang, J.; Feringa, B. L. *Science* **2011**, *331*, 1429–1432.
- (30) Kucharski, T. J.; Boulatov, R. *J. Mater. Chem.* **2011**, *21*, 8237–8255.
- (31) Yang, Q.-Z.; Huang, Z.; Kucharski, T. J.; Khvostichenko, D.; Chen, J.; Boulatov, R. *Nat. Nanotechnol.* **2009**, *4*, 302–306.
- (32) Akbulatov, S.; Tian, Y.; Boulatov, R. *J. Am. Chem. Soc.* **2012**, *134*, 7620–7623.
- (33) Uno, B. E.; Gillis, E. P.; Burke, M. D. *Tetrahedron* **2009**, *65*, 3130–3138.
- (34) Gillis, E. P.; Burke, M. D. *J. Am. Chem. Soc.* **2007**, *129*, 6716–6717.
- (35) Disalvo, E. A.; Simon, S. A. *Permeability and Stability of Lipid Bilayers*; Taylor & Francis: Boca Raton, FL, 1995.
- (36) Kampf, J. P.; Cupp, D.; Kleinfeld, A. M. *J. Biol. Chem.* **2006**, *281*, 21566–21574.
- (37) Quick, M.; Berndt, F.; Dobryakov, A. L.; Ioffe, I. N.; Granovsky, A. A.; Knie, C.; Mahrwald, R.; Lenoir, D.; Ernsting, N. P.; Kovalenko, S. A. *J. Phys. Chem. B* **2014**, *118*, 1389–1402.